



# Unsteady MHD Stagnation Point Flow of $\text{Al}_2\text{O}_3\text{-Cu}/\text{H}_2\text{O}$ Hybrid Nanofluid Past a Convectively Heated Permeable Stretching/Shrinking Sheet with Suction/Injection

Ansab Azam Khan<sup>1</sup>, Khairy Zaimi<sup>2,\*</sup>, Teh Yuan Ying<sup>1</sup>

<sup>1</sup> School of Quantitative Sciences, UUM College of Arts & Sciences, Universiti Utara Malaysia, 06010 UUM Sintok, Kedah Darul Aman, Malaysia

<sup>2</sup> Institute of Engineering Mathematics, Universiti Malaysia Perlis, Pauh Putra Main Campus, 02600 Arau, Perlis, Malaysia

## ARTICLE INFO

### Article history:

Received 15 February 2022

Received in revised form 5 May 2022

Accepted 10 May 2022

Available online 10 June 2022

### Keywords:

Hybrid nanofluid; unsteady stagnation-point; suction/injection; magnetohydrodynamic (MHD); bvp4c

## ABSTRACT

The numerical investigation of unsteady magnetohydrodynamic (MHD) stagnation point flow of  $\text{Al}_2\text{O}_3\text{-Cu}/\text{H}_2\text{O}$  hybrid nanofluid past a convectively heated permeable stretching/shrinking sheet with suction/injection effect is underlined. The characteristic of MHD and boundary condition with suction/injection has received a lot of consideration due to its across-the-board application in mechanical and chemical engineering. The governing continuity, momentum and energy equations are transformed into a system of nonlinear ordinary differential equations using similarity transformation, which is then solved using the bvp4c routine. Numerical results are obtained for the skin friction coefficient, local Nusselt number as well as the velocity and temperature profiles for certain values of the governing parameters, namely suction/injection parameter, copper nanoparticle volume fraction parameter and MHD parameter. Results showed that both velocity profile and temperature increase as the suction/injection parameter  $\gamma$  increases for the first solution and decreases for the second solution. Similarly, when increase the value of MHD parameter  $M$ , the velocity and temperature profiles are decreases for both solutions. The magnitude of the reduced skin friction coefficient and the local Nusselt number are notably increased for the first solution with increasing values of the suction/injection and MHD parameters. Finding also revealed that the skin friction coefficient is intensified in conjunction with the local Nusselt number by adding up the copper nanoparticle volume fraction. In general, dual solutions are found to exist to a particular extent of the stretching/shrinking sheet.

## 1. Introduction

Stagnation points flow is a fundamental phenomenon since it features are linked to all contacts between the flowing fluid and the solid structures. Specifically, such flow is mainly formed by the fluid flows near the stagnating flow of a solid surface in the fluid substance or by fluid dynamics. From the perspective of technical application, it is particularly crucial to determine the rate of variation of physical parameters around the flow environment. The largest heat transfer and highest pressure

\* Corresponding author.

E-mail address: [khairy@unimap.edu.my](mailto:khairy@unimap.edu.my)

<https://doi.org/10.37934/arfmts.96.1.96114>

combined with a velocity decrease occurs in the stagnation point flow around the flow environment. The selection of the working fluid or the form of the solid structure can therefore have a substantial impact on fluid flow and heat transmission. The phenomenon and heat transmission involving stagnation point flow can be observed in many areas such as electronic, hydrodynamic, and aerodynamic. Due to its wide variety of applications, stagnation point flow has been examined by many experts. For instance, Mahapatra and Gupta [1] studied the impact of stretching surface on stagnation point flow. Stretching sheet has numerous essential industrial usages, such as paper manufacturing, polymer sheets, condensed liquid film, and matt fiber [2]. On the other hand, Miklavčič and Wang [3] examined the shrinking surface in which the velocity of the fluid flows on the boundary to a fixed point. They found that such a flow depends on mass suction imposed externally. Afterwards, Wang [4] extended the work of Miklavčič and Wang [3] to the case of stagnation-point flow. He discovered that solutions do not occur for bigger shrinking rates and may be non-unique in the two-dimensional situation. The flow structure is complicated by the non-alignment of the stagnation point flow and the shrinking sheet. Since then, numerous writers have explored extensively the flow caused by stretching/shrinking areas with different geometric structures [5].

Another heat transfer fluid that is thought to have greater heat features than nanofluid and the typical base fluid is hybrid nanofluid. Hybrid nanofluid is a mixture of two different kinds of nanoparticles into a base fluid. Nanoparticles that are commonly employed during the preparation of nanofluid and hybrid nanofluid are metals (i.e., copper (Cu), silver (Ag), nickel (Ni), and gold (Au)), metal oxides (i.e., alumina ( $\text{Al}_2\text{O}_3$ ), hematite ( $\text{Fe}_2\text{O}_3$ ), and tenorite (CuO)), metal carbides, metal nitrides and carbon materials (i.e., carbon nanotubes (CNTs), muti-walled carbon nanotubes (MWCNTs), graphite's, and diamonds.). Ahmed *et al.*, [6] studied the metal oxide and ethylene glycol based well stable nanofluids for mass flow in closed conduit. For the stability of nanofluids, Sajid and Ali [7] determined that the correct selection of the nanoparticles was essential. They also examined the development of hybrid nanofluids and their thermal conductivity. In comparison with the increased heat conduction of single and hybrid nano-additives, while Sarkar *et al.*, [8] addressed about the meaning of the hybridization process. They demonstrated that appropriate hybridization may make hybrid nanofluids extremely attractive for heat transfer improvement. Suresh *et al.*, [9] evaluated the impact on the heat transfer performance of the combined hybrid ( $\text{Al}_2\text{O}_3/\text{H}_2\text{O}$ ) nanofluid. According to the findings of this study, the thermal conductivity and viscosity of the produced hybrid nanofluids increased with the nanoparticles volume concentration. The experimental impact of temperatures and the concentration of particles on hybrid nanofluid dynamic viscosity have been examined by Soltani and Akbari [10]. They used hybrid magnesium oxide (MgO) – MWCNT/ethylene glycol nanofluid. Chamkha *et al.*, [11] and Mehryan *et al.*, [12] examined many elements of fluid flow and heat transfer with Cu-  $\text{Al}_2\text{O}_3/\text{H}_2\text{O}$  hybrid nanofluid. They discovered that the basic  $\text{Al}_2\text{O}_3/\text{H}_2\text{O}$  nanofluid had a higher natural convection heat transfer rate than the Cu- $\text{Al}_2\text{O}_3/\text{H}_2\text{O}$  hybrid nanofluid. The importance of hybrid nanofluid has also examined by Sidik *et al.*, [13], Akilu *et al.*, [14], Babu *et al.*, [15], Sundar *et al.*, [16], Leong *et al.*, [17] and Huminic and Huminic [18].

In addition, numerous investigators have carried out the examination of stretching and shrinking flows with Cu-  $\text{Al}_2\text{O}_3/\text{H}_2\text{O}$  hybrid nanofluid. Devi and Devi [19] have presented a special type of thermophysical characteristics for hybrid nanofluid. According to the findings of this study, the heat transfer rate of the abovementioned hybrid nanofluid is greater than that of Cu/ $\text{H}_2\text{O}$  nanofluid in a magnetic field system. Devi and Devi [20] have addressed the three-dimensional stretching Cu- $\text{Al}_2\text{O}_3/\text{H}_2\text{O}$  hybrid nanofluid flow with magnetic field and convective conditions. They discovered that even in the presence of a magnetic field, the heat transfer rate of the said hybrid nanofluid is faster than that of Cu/ $\text{H}_2\text{O}$  nanofluid. The required heat transfer rate may be obtained by using varied and

suitable nanoparticle proportions in hybrid nanofluid. Hayat and Nadeem [21] have analyzed a three-dimensional Ag-CuO/H<sub>2</sub>O hybrid nanofluid flow across a stretching layer using thermal radiation, chemical reaction, and heat generation. They found that the heat transfer rate of hybrid nanofluid is greater than that of simple nanofluid due to radiation, heat generation, and chemical reaction. Nadeem *et al.*, [22] has investigated the stagnation point flow of Cu- Al<sub>2</sub>O<sub>3</sub>/H<sub>2</sub>O hybrid nanofluid across cylindrical surfaces while Yousefi *et al.*, [23] have examined the stagnation point flow to a wavy cylindrical with TiO<sub>2</sub>-Cu/H<sub>2</sub>O hybrid nanofluid. They noticed that hybrid nanofluid had a higher heat transfer rate than nanofluid. Waini *et al.*, [24] and Khashi'ie *et al.*, [25] subsequently studied the characteristics of the dual solutions of Cu- Al<sub>2</sub>O<sub>3</sub>/H<sub>2</sub>O hybrid nanofluid across linear, exponential, and radially permeable shrinking sheet. The examination of stability was performed, and the first solution was the real solution.

The velocity slip is one of the physical characteristics in boundary layer flow. In some boundary layer flow problems, the use of no-slip condition is unworkable. The slip flow applies in comparison to the zero-slip flow, for the micro and nano-scale system. The boundary layer flow with slip condition to permeable blocks has experimentally examined by Beavers and Joseph [26]. A simple idea is presented and demonstrated to be in fair accord with experimental data by replacing the influence of the boundary layer with a slip velocity proportionate to the external velocity gradient. Andersson [27] and Wang [28] examined the viscous slip-velocity flow along a stretching surface. They discovered an exact similarity solution of the Navier–Stokes equations that may be used to model stretching flow with partial slip. Mahabaleshwar *et al.*, [30] completed recent investigations on boundary layer flow with slip effect using Newtonian fluid. They discovered that Navier's slip condition can cause a non-essential increase in boundary layer thickness as well as a drop in axial and transverse velocities. Rusdi *et al.*, [29] has been examined the thermal radiation in nanofluid penetrable flow bounded with partial slip impact. Ebaid *et al.*, [32] found that the temperature of Cu/H<sub>2</sub>O and TiO<sub>2</sub>/H<sub>2</sub>O nanofluids has increased along with the enhancement of the slip parameter. Stagnation point flow of Williamson nanofluid towards a permeable stretching/shrinking sheet with partial slip effect has been examined by Khan *et al.*, [31]. The velocity profile has also improved by raising the velocity slip parameter as discussed by Bhattacharya *et al.*, [33] and Aziz *et al.*, [34].

In aerodynamics and space physics, it has been stated that suction and injection played significant role in controlling the flux on the supersonic aircraft surface [35]. Suction and injection of a fluid by the joining layer will affect the flow field dramatically. Suction generally increases the skin friction, while injection works in the opposite manner. Suction and injection have performed a vital role in engineering such as high-temperature analysis, electrical stainless steel, and the petrochemical industry. Many researchers such as Bachok *et al.*, [36], Rehman *et al.*, [37] and Li *et al.*, [38] have recently studied the effects of suction and injection on various forms of fluid flows over an exponential shrinking sheet with stability analysis. Suction delayed the boundary layer separation, whereas injection enhances it, according to their findings. Anuar *et al.*, [39] evaluated the effect of suction and injection on stagnation point flow of hybrid nanofluid. They showed that the suction variable has a greater influence on skin friction and heat transmission than the injection variable. Recently, an unsteady MHD stagnation point flow over an exponential permeable stretching and shrinking sheet of hybrid nanofluid, was explored by Zainal *et al.*, [40]. In this research, they observed that both local Nusselt number and skin friction coefficient has improved along with the suction/injection parameter. Since the heat transfer and fluid flow problems are very comprehensive in manufacturing processes where suction and injection results are included, the current study may have a significant influence on the heat transfer mechanism.

The study of the phenomenon of magnetohydrodynamics (MHD) flow has received significant attention due to its practical usage in fusion reactors, fibre optic filters, crystal growth, metal casting,

and optical greasing, to name a few [41]. The existence of MHD in conduction fluid causes motion resistance of the fluid particles and this can be defined as Lorentz force. Lorentz force greatly increases with the density and fluid temperature, hence delays the boundary layer separation [42]. In consideration of the effects from thermophoresis and Brownian motion, Tian *et al.*, [43] provided numerical research on a MHD and convective stagnation-point nanofluid flow. They examined the impact of the magnetic field, Prandtl number, viscous dissipation, Lewis number, heat source/sink with suction/injection, Brownian motion parameter and thermophoresis parameters on the thermal boundary layer and flow field, along with Nusselt number, skin friction coefficient, and Sherwood number. In another study, Dhanai *et al.*, [44] examined a MHD boundary layer nanofluid flow with viscous dissipation passes through a power-law permeable sheet, where they found out the presence of dual solutions with respect various stretching/shrinking parameter. The study of slip, chemical reaction, and Joule heating effects on magnetohydrodynamic nanofluid and hybrid nanofluid has been conducted by Khan *et al.*, [45,46], Ashgar and Ying [47] and Akaje and Olajuwon [48]. The examination on an unsteady MHD flow at the forward stagnation-point was first prompted by Katagiri [49], Pavlov [50] and Takhar *et al.*, [51]. They inspected the stability of the solution and reported that their work was extended by an investigation into the electrically conducting fluid of the MHD boundary layer with a transversal magnetic field due to the stretching surface. Since then, a huge proportion of research have been published in several aspects including MHD on the stretching/shrinking surface and heat transfer, notably from the works of Zainal *et al.*, [52], Jamaludin *et al.*, [53] and Mallick and Misra [54]. They demonstrated that the presence of a magnetic field and suction would slow down the fluid's velocity due to the synchronization of the magnetic and electric fields caused by the creation of the Lorentz force.

As far as the investigators' knowledge, existing literature did not take into consideration the unsteady stagnation points flow of hybrid nanofluid with the inclusion of suction/injection and magnetic field into the physical model. Thus, this research gap motivated the investigators to conduct a heat transfer analysis on an unsteady stagnation point flow which passes through a heated stretching/shrinking sheet involving alumina-copper/water ( $\text{Al}_2\text{O}_3\text{-Cu}/\text{H}_2\text{O}$ ) with the influence of MHD and suction/injection. In many engineering challenges including start-up and regular fluid motion, unsteady boundary layer flow plays a significant role. The behavior of unsteady boundary layer flow is different from its steady counterpart because it has additional time-dependent element which affect the fluid motion pattern and the separation of the boundary layer [55]. The hybrid nanofluid is prepared by dispersal of the  $\text{Al}_2\text{O}_3$  nanoparticles into  $\text{H}_2\text{O}$ , accompanied with Cu with different volume fractions. The thermophysical properties of the hybrid nanofluid are adopted from Takabi and Salehi [56] and Ghalambaz *et al.*, [57]. The pre-built *bvp4c* numerical algorithm which runs on MATLAB is used for the numerical computations. Discussion on the findings of reduced skin friction coefficient, local Nusselt number, velocity profile, and temperature profile in terms of suction/injection, MHD and nanoparticles volume fraction are carried out. Particular cases of the present study are compared with those of Zainal *et al.*, [58]. All results obtained in this study are original and new.

## 2. Mathematical Model

In this study, as shown in Figure 1, we consider the unsteady two-dimensional MHD stagnation-point flow for  $\text{Al}_2\text{O}_3\text{-Cu}/\text{H}_2\text{O}$  hybrid nanofluid over a convectively heated stretching/shrinking sheet with suction/injection [59]. The stretching/shrinking velocity is denoted by  $u_w(x, t) = bx/(1 - ct)$ , where  $b$  denotes a constant corresponds to stretching ( $b > 0$ ) and shrinking ( $b < 0$ ) cases while  $c$  signifies the unsteady flow and  $u_e(x, t) = ax/(1 - ct)$  is the velocity of the free stream where  $a >$

0 represents the strength of the stagnation flow. The ambient temperature and the reference temperature are  $T_\infty$  and  $T_0$ , respectively. Now, we let the bottom of the sheet be heated by convection from a hot fluid at a specific temperature  $T_f(x, t) = T_\infty + T_0 \frac{ax}{2v} (1 - ct)^{-3/2}$ . From all of the assumptions above, the governing boundary layer equations can be given as follows

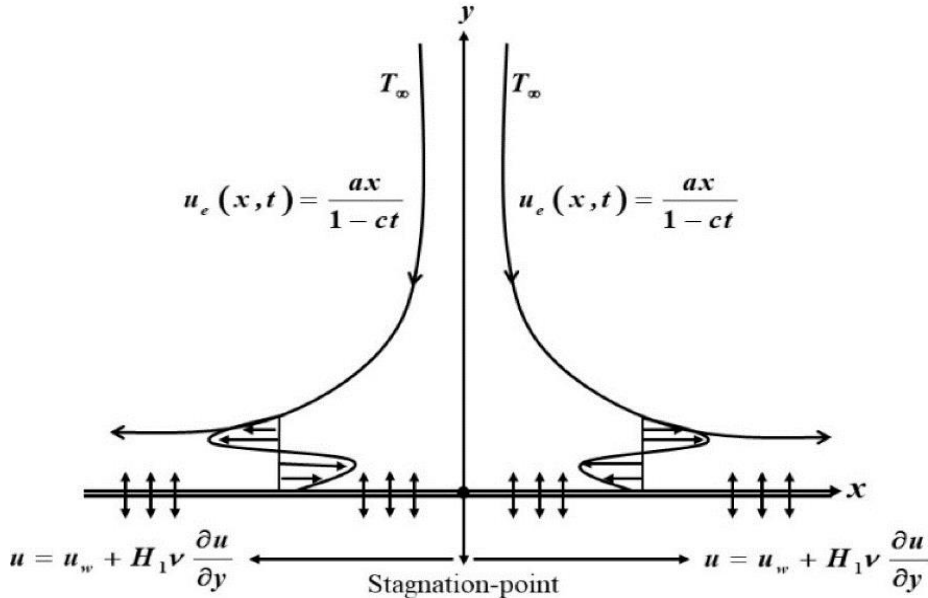


Fig. 1. The schematic of problem flow [52]

$$\frac{\partial u}{\partial x} + \frac{\partial v}{\partial y} = 0 \quad (1)$$

$$\frac{\partial u}{\partial t} + u \frac{\partial u}{\partial x} + v \frac{\partial u}{\partial y} = \frac{\partial u_e}{\partial t} + u_e \frac{\partial u_e}{\partial x} + \frac{\mu_{hnf}}{\rho_{hnf}} \frac{\partial^2 u}{\partial y^2} - \frac{\sigma_{hnf}}{\rho_{hnf}} B_0^2 u \quad (2)$$

$$\frac{\partial T}{\partial t} + u \frac{\partial T}{\partial x} + v \frac{\partial T}{\partial y} = \frac{k_{hnf}}{(\rho C_p)_{hnf}} \frac{\partial^2 T}{\partial y^2} \quad (3)$$

where  $T$  is the temperature, as well as  $u$  and  $v$  being the velocity components along the  $x$ -axis and  $y$ -axis, respectively. Furthermore,  $\mu_{hnf}$  is the dynamic viscosity,  $\rho_{hnf}$  is the density,  $k_{hnf}$  is the thermal conductivity, and  $(\rho C_p)_{hnf}$  is the heat capacity of  $Al_2O_3$ -Cu/ $H_2O$  hybrid nanofluid. The boundary conditions with the partial slip and suction/injection are set to be

$$u = u_w(x, t) + H_1 v \frac{\partial u}{\partial y}, v = v_w, -k_{hnf} \frac{\partial T}{\partial y} = h_f + (T_f - T) \text{ at } y = 0 \quad (4)$$

$$u \rightarrow u_e(x, t), T \rightarrow T_\infty, \text{ as } y \rightarrow \infty$$

where  $H_1 = H(1 - ct)^{1/2}$  is the velocity slip factor, in which  $H$  refers to the initial value of the velocity slip factor. The physical properties of copper (Cu), alumina ( $Al_2O_3$ ) and water ( $H_2O$ ) are provided in Table 1. In the meantime, Table 2 showed the thermophysical properties of  $Al_2O_3$ -Cu/ $H_2O$  hybrid nanofluid. The nanoparticles solid volume fraction is represented by  $\phi$ ,  $\rho_f$  indicates the density of base fluid ( $H_2O$ ),  $\rho_s$  is the density of the hybrid nanoparticle,  $C_p$  is the heat capacity at constant pressure, while  $k_f$  denotes the thermal conductivity of base fluid ( $H_2O$ ) and  $k_s$  is the hybrid nanoparticle thermal conductivity. Supplies coefficient of heat transfer is expressed by  $h_f$ .

**Table 1**  
 Thermophysical properties of Cu, Al<sub>2</sub>O<sub>3</sub> and H<sub>2</sub>O [64]

Properties	k (W/mK)	ρ (kg/m <sup>3</sup> )	C <sub>p</sub> (J/kgK)	β × 10 <sup>-5</sup> (mK)
Cu	400	8933	385	1.67
Al <sub>2</sub> O <sub>3</sub>	40	3970	765	0.85
H <sub>2</sub> O	0.613	997.1	4179	21

**Table 2**  
 Thermophysical properties of hybrid nanofluid [56,57]

Properties	Hybrid Nanofluid
Dynamic viscosity	$\mu_{hnf} = \frac{1}{(1 - \phi_{hnf})^{2.5}}$
Density	$\rho_{hnf} = (1 - \phi_{hnf})\rho_f + \phi_1\rho_{s1} + \phi_2\rho_{s2}$
Thermal capacity	$(\rho C_p)_{hnf} = (1 - \phi_{hnf})(\rho C_p)_f + \phi_1(\rho C_p)_{s1} + \phi_2(\rho C_p)_{s2}$
Thermal conductivity	$\frac{k_{hnf}}{k_f} = \left[ \frac{(\frac{\phi_1 k_{s1} + \phi_2 k_{s2}}{\phi_{hnf}}) + 2k_f + 2(\phi_1 k_{s1} + \phi_2 k_{s2}) - 2\phi_{hnf} k_f}{(\frac{\phi_1 k_{s1} + \phi_2 k_{s2}}{\phi_{hnf}}) + 2k_f - (\phi_1 k_{s1} + \phi_2 k_{s2}) + \phi_{hnf} k_f} \right]$

In order to express the governing Eq. (1) to Eq. (3) and boundary conditions (4) in a much simpler form, the subsequent similarity transformations are considered [60]

$$\psi = \left(\frac{av}{1-ct}\right)^{\frac{1}{2}} xf(\eta), \theta(\eta) = \frac{T-T_\infty}{T_f-T_\infty}, \eta = \left(\frac{a}{v(1-ct)}\right)^{1/2} y \tag{5}$$

where  $\psi$  is the stream function which can be specified as  $u = \partial\psi/\partial y$  and  $v = -\partial\psi/\partial x$ , while  $\eta$  is the similarity variable. Thus, we attain

$$u = \frac{ax}{(1-ct)} f'(\eta) \text{ and } v = \left(\frac{av}{1-ct}\right)^{\frac{1}{2}} f(\eta). \tag{6}$$

By employing the similarity variables (5) and (6), the governing Eq. (2) and Eq. (3) can be reduced to the following system of nonlinear ordinary differential equations (ODEs)

$$\frac{\mu_{hnf}/\mu_f}{\rho_{hnf}/\rho_f} f''' + ff'' - f'^2 + 1 - \varepsilon \left(f' + \frac{1}{2}\eta f'' - 1\right) - \frac{\sigma_{hnf}/\sigma_f}{\rho_{hnf}/\rho_f} M f' = 0 \tag{7}$$

$$\frac{1}{Pr} \frac{k_{hnf}/k_f}{(\rho C_p)_{hnf}/(\rho C_p)_f} \theta'' + f\theta' - 2f'\theta + \frac{\varepsilon}{2}(\eta\theta' + 3\theta) = 0 \tag{8}$$

Here,  $\lambda$  measures the unsteadiness parameter with  $\lambda = c/a$ , and  $Pr = (\mu c_p)_f/k_f$  represents the Prandtl number. Next, the boundary conditions (4) can now be transformed into

$$f(0) = \gamma, f'(0) = \varepsilon + \delta f''(0), -\frac{k_{hnf}}{k_f} \theta'(0) = Bi[1 - \theta(0)], \tag{9}$$

$$f'(\eta) \rightarrow 1, \theta(\eta) \rightarrow 0 \text{ as } \eta \rightarrow \infty.$$

From Eq. (9),  $\varepsilon$  symbolized the ratio of velocity parameter,  $M$  is the MHD parameter, as well as  $\sigma$ ,  $\gamma$ , and  $Bi$  being the dimensionless partial slip, suction/injection, and Biot number parameters, as shown below

$$\varepsilon = \frac{b}{a}, M = \frac{B_0^2 ax}{1-ct}, v_w = -\left(\frac{av}{1-ct}\right)^{1/2}, S, \sigma = H(av)^{1/2}, Bi = \frac{h_f}{k_f} \sqrt{\frac{v(1-ct)}{a}}. \quad (10)$$

Next, the skin friction coefficient  $C_f$  and the local Nusselt number  $Nu_x$  are defined as follows

$$C_f = \frac{\tau_w}{\rho_f u_e^2}, Nu_x = \frac{xq_w}{k_f(T_f - T_\infty)}. \quad (11)$$

The shear stress is expressed by  $\tau_w$  along the  $x$ -axis when  $q_w$  signifies the surface heat flux that accentuated by

$$\tau_w = \mu_{hnf} \left(\frac{\partial u}{\partial y}\right)_{y=0}, q_w = -k_{hnf} \left(\frac{\partial T}{\partial y}\right)_{y=0}. \quad (12)$$

By applying Eq. (5) and Eq. (12) into Eq. (11), we acquired

$$\sqrt{Re_x} C_f = \frac{\mu_{hnf}}{\mu_f} f''(0), \frac{1}{\sqrt{Re_x} Nu_x} = -\frac{k_{hnf}}{k_f} \theta'(0) \quad (13)$$

provided that  $Re_x = \frac{\mu_e x}{\nu_f}$  is the local Reynolds number along  $x$ - axis.

### 3. Numerical Method: Bvp4c Solver

The unsteady MHD stagnation point flow of hybrid nanofluid past a convectively heated permeable stretching/shrinking sheet with suction/injection effect is investigated using appropriate governing equations given by Eq. (2) and Eq. (3). The governing equations in Eq. (2) and Eq. (3) are partial differential equations (PDEs) that need to be reduced to a system of nonlinear ODEs in Eq. (7) and Eq. (8) by non-dimensional similarity transformation and solved using bvp4c solver in MATLAB. The reduction to system of ODEs is to make it less intricate in finding numerical solution. Shampine *et al.*, [61] presented this MATLAB solver bvp4c routine which involves finite-difference code that executes the three-stage fourth order Lobatto IIIA formula. The detail execution of the bvp4c for the current problem is presented as follows.

STEP 1: Introduce the following new variables for the system of higher order nonlinear ODES in Eq. (7) and Eq. (8)

$$y(1) = f, y(2) = f', y(3) = f'', y(4) = \theta, y_5 = \theta'. \quad (14)$$

STEP 2: Transform the system of higher order nonlinear ODEs (7) – (8) to a system of first order ODEs

$$\begin{aligned}
 f' &= y(2) \\
 f'' &= y(3) \\
 f''' &= (y(2))^2 - y(1)y(3) - 1 + \varepsilon \left( y(2) + \frac{1}{2}\eta y(3) - 1 \right) - \frac{\sigma_{hnf}/\sigma_f}{\rho_{hnf}/\rho_f} M y(2) \frac{\rho_{hnf}/\rho_f}{\mu_{hnf}/\mu_f} \\
 \theta' &= y(5) \\
 \theta'' &= (2y(2)y(4) - y(1)y(5) - \frac{\varepsilon}{2}(\eta y(5) + 3y(4))) \frac{Pr^{(\rho C_p)_{hnf}}/(\rho C_p)_f}{k_{hnf}/k_f}
 \end{aligned} \tag{15}$$

STEP 3: Transform the boundary conditions (9) using according to new variables introduced in Eq. (14).

$$Y_a(1) = \gamma, Y_a(2) = \lambda + \delta f''(0), -\frac{k_{hnf}}{k_f} Y_a(5) = Bi[1 - Y_a(4)], Y_b(2) = 1, Y_b(4) = 0. \tag{16}$$

Here, the subscript *a* represents the position on the sheet at  $\eta=0$  and subscript *b* represents the position far from the sheet for a particular value of  $\eta$ . In this study, it is sufficient to acquire the correct numerical solution by setting  $\eta = 8$ .

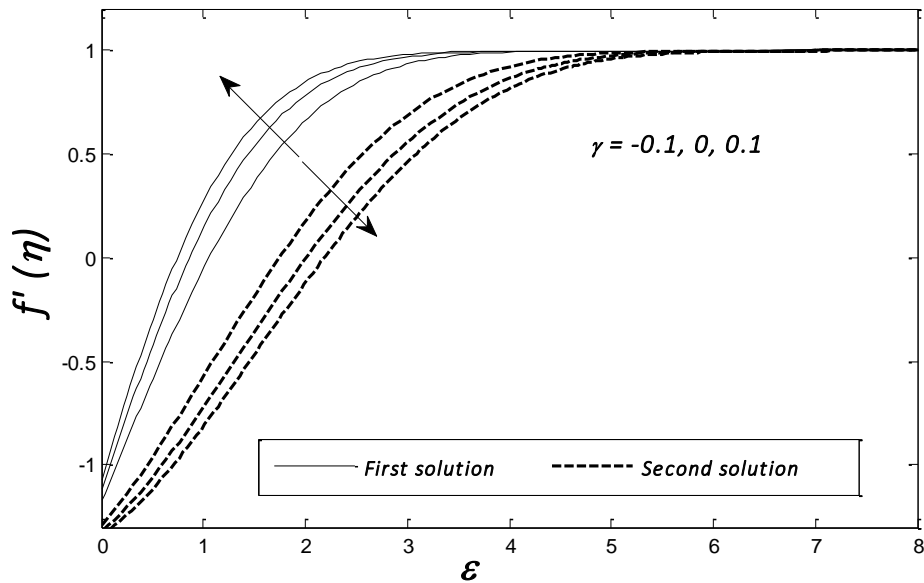
STEP 4: Write the system of first order ODEs (15) with boundary conditions (16) in MATLAB software using `bvp4c` solver to obtain dual solutions. The dual solutions were obtained by setting different initial guesses for  $f''(0)$  and  $\theta'(0)$ , where all profiles satisfy the far-field boundary conditions (9) asymptotically. Convergence of the first solution is usually guaranteed even for poor initial guesses but this is contrary to the initial guesses for the second solution.

#### 4. Results and Discussion

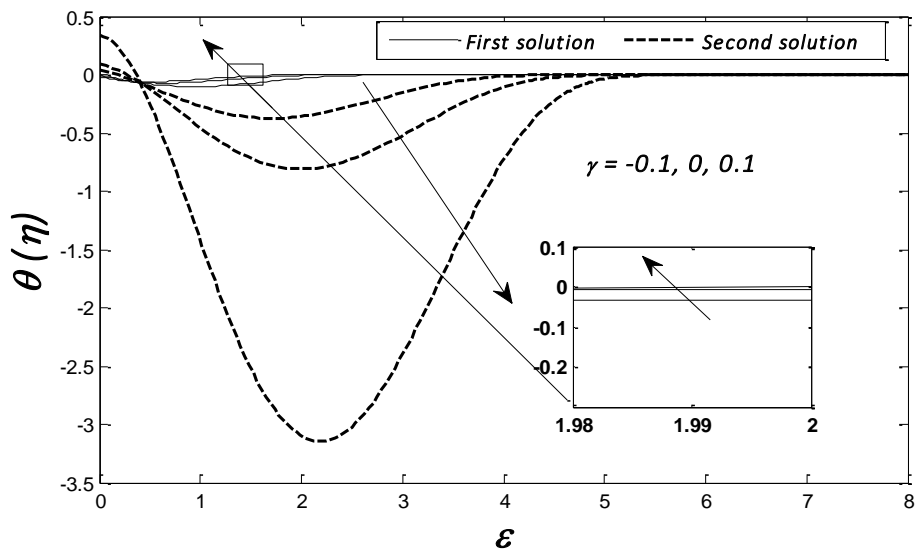
A `bvp4c` approach is a remarkable and thoroughly developed instrument to address the boundary value problems. Early calculation of the primary mesh points and the varying step dimensions are essential to ensure the required results. It is essential to confirm that the diffusion of distinct nanoparticles  $Al_2O_3$  and  $Cu$  is adequate of establishing  $Al_2O_3-Cu/H_2O$  hybrid nanofluid and  $Cu/H_2O$  nanofluid. Aside from that, the Prandtl number (*Pr*) is set to be fixed at  $Pr = 6.2$  which coincide to water as the reference base fluid, while as for the  $Al_2O_3-Cu/H_2O$  hybrid nanofluid, the size of the nanoparticles is assumed to be regulated, and the thermophysical properties impact of nanoparticles is ignored. The following values of the leading parameters were used for this numerical analysis: Prandtl number ( $Pr = 6.2$ ), suction/injection parameter ( $\gamma = -0.1, 0, 0.1$ ), alumina volume fraction ( $\phi_1 = 0.02$ ), unsteadiness parameter ( $\lambda = 0.1$ ), MHD parameter ( $M = 0, 0.01, 0.02$ ), Biot number ( $Bi = 0.2$ ), velocity slip parameter ( $\sigma = 0.2$ ) and copper volume fraction ( $\phi_2 = 0.02, 0.05, 0.08$ ). The emphases were focused on the impact of the suction/injection parameter, MHD parameter, and copper volume fraction on the velocity and heat transfer of the fluid flow, and the skin friction and local Nusselt number, as depicted in Figure 2 to Figure 13.

Figure 2 showed the existence of dual velocity profiles ( $f'(\eta)$ ) with respect to different values of suction/injection parameter ( $\gamma$ ). The first solution increases in proportion to the rise in  $\gamma$ , while the second solution shows contradictory effects from the first solution, presumably due to the improvement in unsteady flow. Similar trend of the solution found in Figure 2 was also reflected in

the temperature distribution  $\theta(\eta)$  as depicted in Figure 3. Obviously, the rate of heat transfer in the first solution is ascending, while the second solution allows a top-down direction when suction/injection is enlarged.



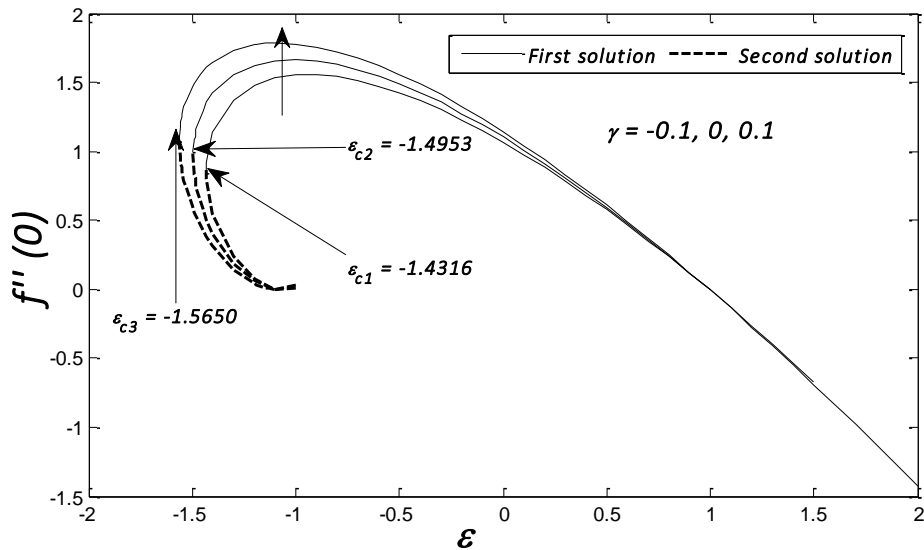
**Fig. 2.** The velocity profiles  $f'(\eta)$  for different values of  $\gamma$  when  $Pr = 6.2, Bi = 0.2, \lambda = 0.1, M = 0.01, \phi_1 = \phi_2 = 0.02, \sigma = 0.2$  and  $\varepsilon = -1.4$  (shrinking case)



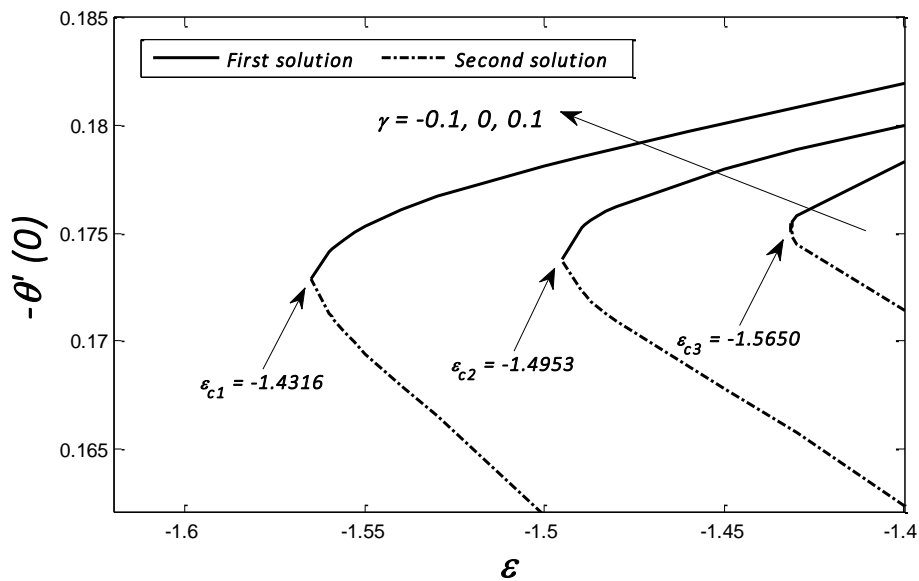
**Fig. 3.** The temperature profiles  $\theta(\eta)$  for different values of  $\gamma$  when  $Pr = 6.2, Bi = 0.2, \lambda = 0.1, M = 0.01, \phi_1 = \phi_2 = 0.02, \sigma = 0.2$  and  $\varepsilon = -1.4$  (shrinking case)

Figure 4 and Figure 5 demonstrated that the distribution of disburse suction/injection parameter in the current study is able to form the dual similarity solutions in both skin friction and Nusselt number. Based on these two figures, dual solutions occurred when  $\varepsilon_c \leq \varepsilon$ , while no solution was found for  $\varepsilon < \varepsilon_c$ . Figure 4 also highlighted as the sheet is stretching at the rate of  $\varepsilon = 1$ , the value of skin friction  $f''(0) = 0$  which characterized as no frictional drag being expanded at the convectively heated stretching/shrinking sheet. It can also be noticed that as the suction/injection impact becomes higher, the range of solutions becomes wider. It is clearly illustrated in Figure 4 that an

increment of  $\gamma$  would increase the value of skin friction ( $f'(\eta)$ ) in the first solution but opposite behaviour is noticed in the second solution.



**Fig. 4.** Variation of skin friction  $f''(0)$  for different values of  $\gamma$  when  $Pr = 6.2, Bi = 0.2, \lambda = 0.1, \phi_1 = \phi_2 = 0.02, \sigma = 0.2$  and  $M = 0.01$



**Fig. 5.** Variation of local Nusselt number  $-\theta'(0)$  for different values of  $\gamma$  when  $Pr = 6.2, Bi = 0.2, \lambda = 0.1, \phi_1 = \phi_2 = 0.02, \sigma = 0.2$  and  $M = 0.01$

Figure 5 exposed an upward trend in Nusselt number ( $-\theta'(0)$ ) when the suction/injection parameter rises on the convectively heated stretching/shrinking sheet, which is proportionate to the heat transfer rate. These results are consistent with Zainal *et al.*, [58]. Obviously, the heat transfer rate for the first solution presents an increasing upward trend, while the second solution allows a top-down trend as the range of suction/injection parameter is widened. Thus, the suction/injection greatly improved the heat transfer rate. The critical values at  $\gamma = -0.1, 0, 0.1$  are  $\epsilon_c = -1.4316, -1.4953, -1.5650$ , respectively. Note that there is no solution for  $\epsilon < \epsilon_c$ .

In Figure 6 and Figure 7, the velocity profile ( $f'(\eta)$ ) and temperature profile ( $\theta(\eta)$ ) with varying values of  $M = 0, 0.01$  and  $0.02$  are seen. As shown in Figure 6, the fluid velocity decreases in both first and second solutions and the transportation rate decrease significantly with increasing value of

$M$ . Consequently, the temperature profile decreases as the magnetohydrodynamic number increases (see Figure 7). This is due to the fact that Lorentz force from the magnetic field induced further transport resistance, thus reduces the shear stress on the floor [62].

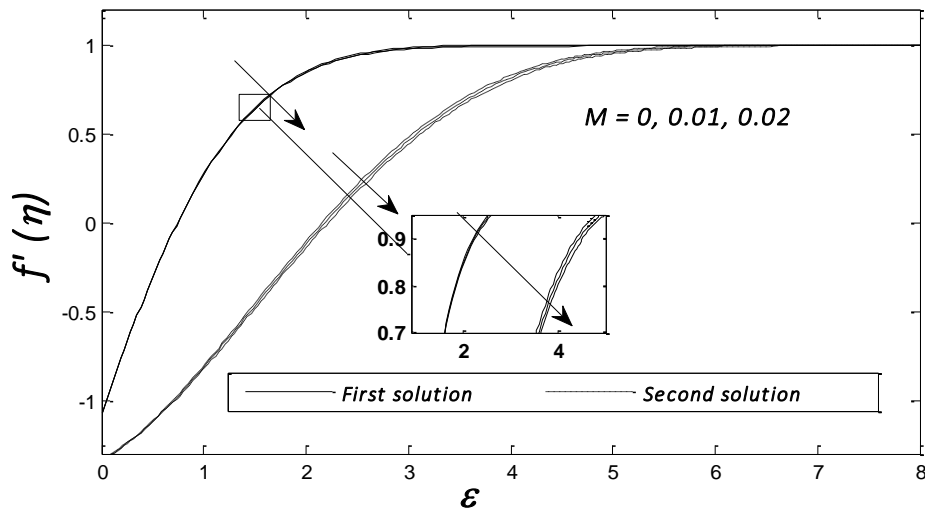


**Fig. 6.** The velocity profiles  $f'(\eta)$  for different values of  $M$  when  $Pr = 6.2, Bi = 0.2, \lambda = 0.1, \gamma = 0.1, \phi_1 = \phi_2 = 0.02, \sigma = 0.2$  and  $\varepsilon = -1.4$  (shrinking case)

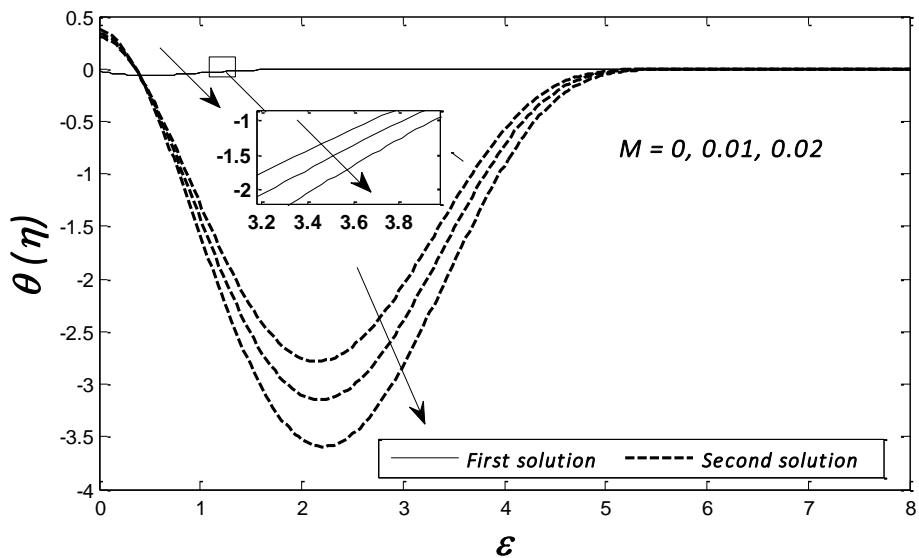


**Fig. 7.** The temperature profiles  $\theta(\eta)$  for different values of  $M$  when  $Pr = 6.2, Bi = 0.2, \lambda = 0.1, \gamma = 0.1, \phi_1 = \phi_2 = 0.02, \sigma = 0.2$  and  $\varepsilon = -1.4$  (shrinking case)

The effect of  $M$  on the variations of skin friction ( $f''(0)$ ) and Nusselt number ( $-\theta'(0)$ ) with respect to  $\varepsilon$  when  $Pr = 6.2, Bi = 0.2, \lambda = 0.1, \phi_1 = \phi_2 = 0.02, \sigma = 0.2$  and  $\gamma = 0.1$  are presented in Figure 8 and Figure 9, respectively. It is found that that the presence of  $M$  causes the partition of the boundary layer, where the critical values of  $\varepsilon_c$  slightly moved to the left. This was when the Lorentz force prevented the rotational velocity of the sheet within the boundary layer. In addition, the values of skin friction ( $f''(0)$ ) and Nusselt number ( $-\theta'(0)$ ) increases as the values  $M$  for the first solution is enhanced but an opposite pattern is observed in the second solution The dual solutions are

achieved for  $\varepsilon > \varepsilon_c$ , where the critical values at different stages of  $M = 0, 0.01, 0.02$  are  $\varepsilon_c = -1.5620, -1.5651, -1.5657$ , respectively. No solution exists when  $\varepsilon < \varepsilon_c$ .

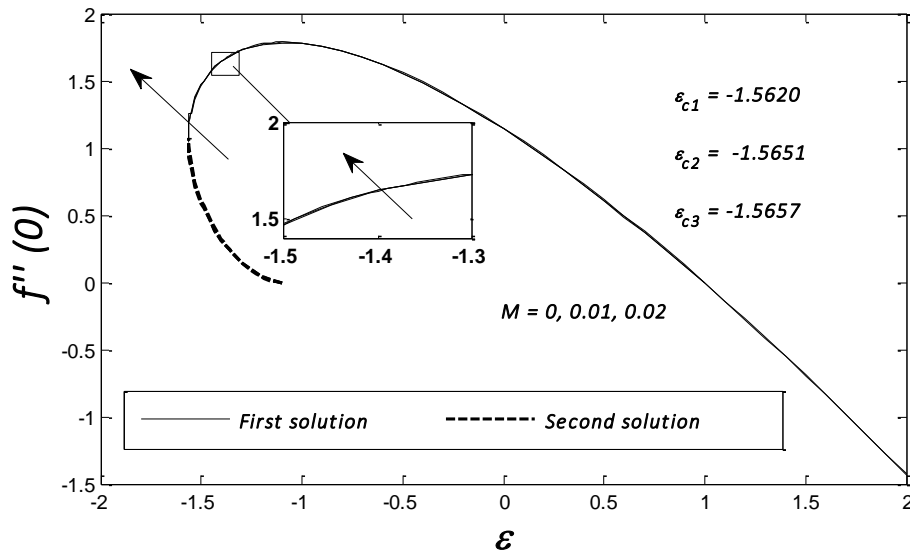


**Fig. 8.** Variation of skin friction  $f''(0)$  for different values of  $M$  when  $Pr = 6.2, Bi = 0.2, \lambda = 0.1, \phi_1 = \phi_2 = 0.02, \sigma = 0.2$  and  $\gamma = 0.1$

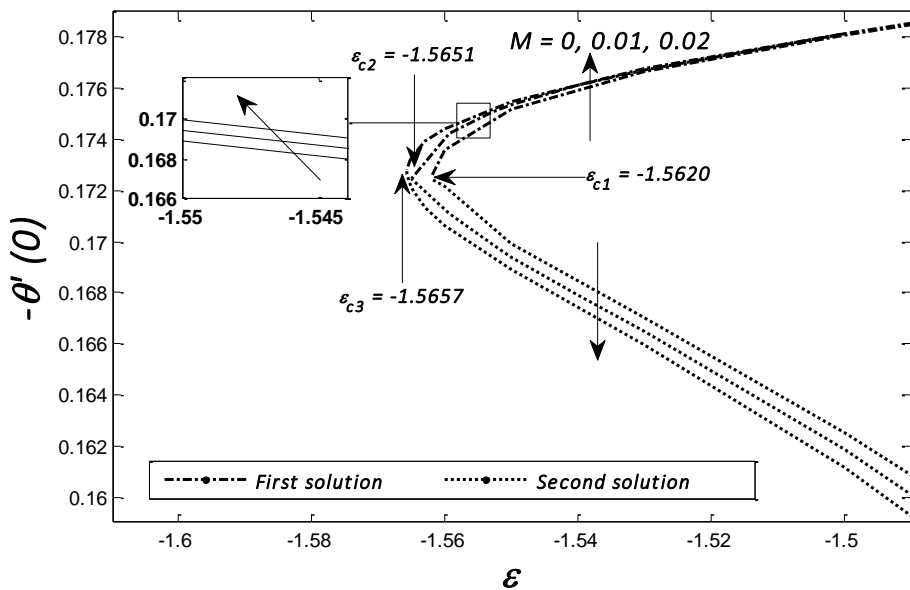


**Fig. 9.** Variation of local Nusselt number  $-\theta'(0)$  for different values of  $M$  when  $Pr = 6.2, Bi = 0.2, \lambda = 0.1, \phi_1 = \phi_2 = 0.02, \sigma = 0.2$  and  $\gamma = 0.1$

The viscosity of  $Al_2O_3-Cu/H_2O$  hybrid nanofluid rises when  $\phi_2$  increases, which eventually improves the fluid velocity over the convectively heated shrinking sheet, as shown in Figure 10. The velocity profile in Figure. 10 clarifies that the momentum boundary layer thickness has diminished in response to the rise of  $\phi_2$ , thereby raising the velocity of the fluid and boosting the gradient of velocity. The temperature profile in Figure 11 shows the temperature variations where both first and second solutions increases when the value of  $\phi_2$  is rises. The results obtained in Figure 10 and Figure 11 are consistent with Zainal *et al.*, [40] whereby adding the concentrations of hybrid nanoparticles may contribute to the improvement of the heat transfer rate.

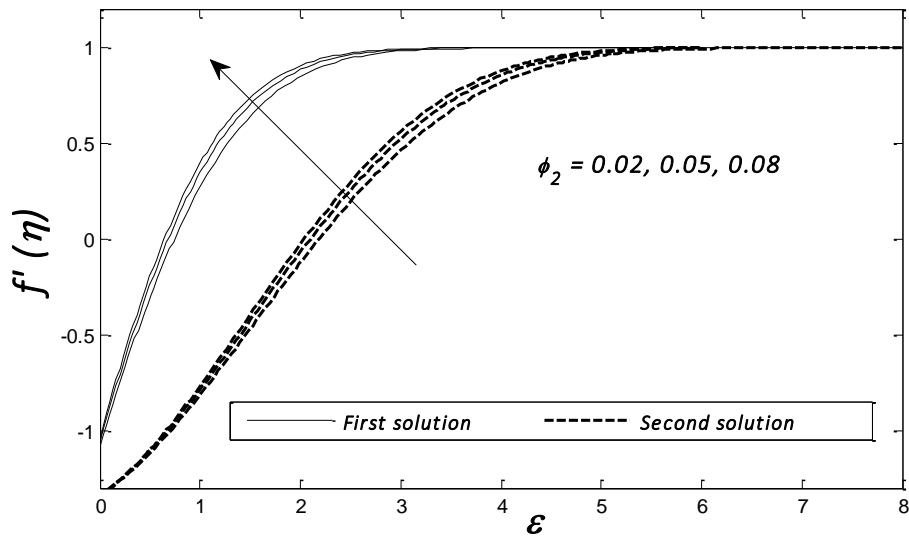


**Fig. 10.** The velocity profiles  $f'(\eta)$  for different values of  $\phi_2$  when  $Pr = 6.2, Bi = 0.2, \lambda = 0.1, M = 0.01, \phi_1 = 0.02, \sigma = 0.2, \gamma = 0.1$  and  $\varepsilon = -1.4$  (shrinking case)

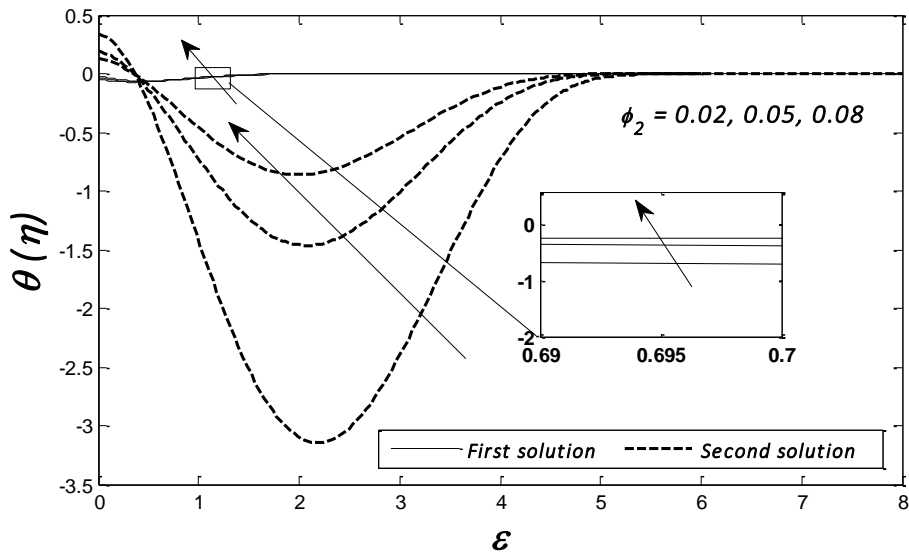


**Fig. 11.** The temperature profiles  $\theta(\eta)$  for different values of  $\phi_2$  when  $Pr = 6.2, Bi = 0.2, \lambda = 0.1, \gamma = 0.1, \phi_1 = 0.02, \sigma = 0.2, M = 0.01$  and  $\varepsilon = -1.4$  (shrinking case)

Figure 12 and Figure 13 showed the influence of the nanoparticle volume fraction of alumina ( $\phi_1$ ) and copper ( $\phi_2$ ) on the skin friction ( $f''(0)$ ) and Nusselt number ( $-\theta'(0)$ ), when  $\phi_1$  is set to 0.02 and  $\phi_2$  varies in several values ( $\phi_2 = 0.02, 0.05, 0.08$ ). It is obvious from Figure 12 that for an increasing  $\phi_2$ , the deviations from the skin friction ( $f''(0)$ ) to  $\varepsilon$  for the first solution has increased but found reduced for the second solution. On the other hand, Nusselt number ( $-\theta'(0)$ ) has decreased for both first and second solutions, as shown in Figure 13. This finding is consistent with the fact that by including hybrid nanoparticles, the heat transfer rate increases due to the synergistic effects described by Sarkar *et al.*, [63]. Based on our computations, the critical values of  $\varepsilon = \varepsilon_c$  for  $\phi_2 = 0.02, 0.05$  and  $0.08$  are  $\varepsilon_c = -1.5651, -1.5776$  and  $-1.5899$ , respectively. Note that no solution exists when  $\varepsilon < \varepsilon_c$ .

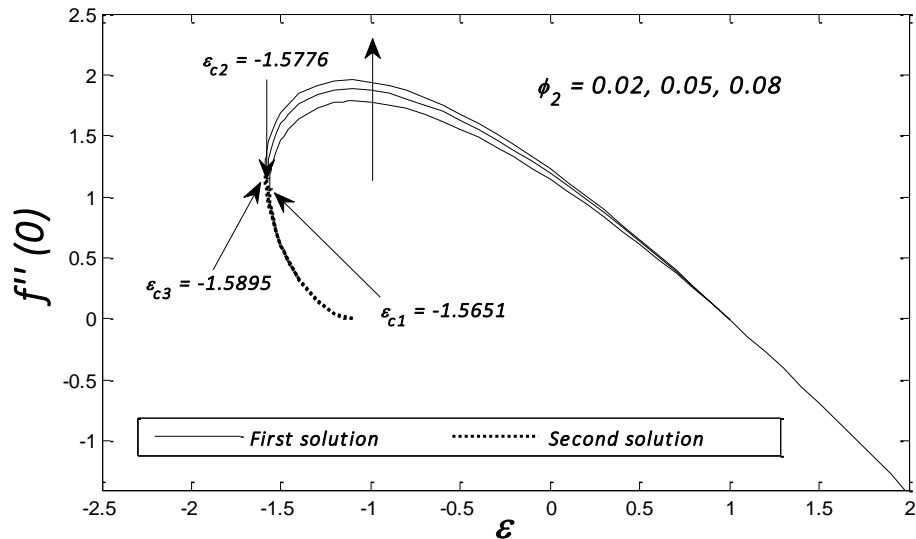


**Fig. 12.** Variation of skin friction  $f''(0)$  for different values of  $\phi_2$  when  $Pr = 6.2, Bi = 0.2, \lambda = 0.1, \phi_1 = 0.02, \sigma = 0.2, M = 0.01$  and  $\gamma = 0.1$

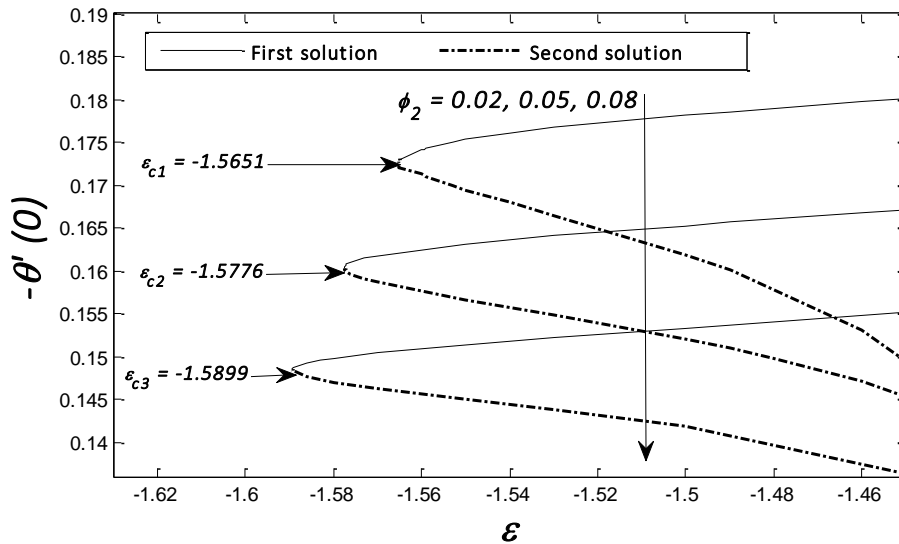


**Fig. 13.** Variation of local Nusselt number  $-\theta'(0)$  for different values of  $\phi_2$  when  $Pr = 6.2, Bi = 0.2, \lambda = 0.1, \phi_1 = 0.02, \sigma = 0.2, M = 0.01$  and  $\gamma = 0.1$

Table 3 has validated those current numerical results is consistent with previously reported results by Zainal *et al.*, [58] on the values of skin friction and local Nusselt number for normal fluid ( $\phi_1 = \phi_2 = 0$ ) when  $M = Bi = \sigma = \gamma = \lambda = 0$ . Additionally, the numerical values of skin friction ( $f''(0)$ ) and local Nusselt number ( $-\theta'(0)$ ) for different values of  $M$  and  $\gamma$  were presented in Table 4 and Table 5. The smallest eigenvalues  $\omega_1$  for particular values of  $\varepsilon$  when  $Pr = 6.2, Bi = 0.2, \lambda = 0.1, M = 0.01, \phi_1 = \phi_2 = 0.02, \sigma = 0.2$  with  $\gamma = -0.1, 0, 0.1$  are tabulated in Table 6. The values of  $\omega_1$  in the first are seen to be close to zero for  $\varepsilon \rightarrow \varepsilon_c$  in chosen cases of  $\gamma$  and the values of second solution are increases.

**Table 3**

Evaluation of  $f''(0)$  when  $\gamma = \sigma = Bi = M = \lambda = 0$  by certain values of  $\varepsilon$

$\varepsilon$	Present Result		Zainal <i>et al.</i> , [58]	
	First solution	Second solution	First solution	Second solution
-0.25	1.402241	-	1.402241	-
-0.60	1.507024	-	-	-
-0.85	1.448944	-	-	-
-1.00	1.328817	0.000000	1.328817	0.000000
-1.15	1.082231	0.116702	1.082231	0.116702
-1.24	0.706605	0.435672	-	-
-1.243	0.670429	0.470135	-	-
-1.246	0.609826	0.529035	0.609826	0.529035
-1.2465	0.584282	0.554296	-	-
-1.25	0.580437	0.583055	-	-

**Table 4**

Results of skin friction coefficient ( $f''(0)$ ) and local Nusselt number ( $-\theta'(0)$ ) for different values of  $\gamma$  when  $Pr = 6.2, Bi = 0.2, \lambda = 0.1, M = 0.01, \phi_1 = \phi_2 = 0.02, \sigma = 0.2$  and  $\varepsilon = -1.4$  (shrinking case)

$\gamma$	$f''(0)$	$-\theta'(0)$
-0.1	1.138083143(0.547584054)	0.178307707(0.171404345)
0	1.421749593(0.403945853)	0.180029465(0.162283537)
0.1	1.645073314(0.316328235)	0.181945448(0.118217285)

Note: () Second solution

**Table 5**

Results of skin friction coefficient ( $f''(0)$ ) and local Nusselt number ( $-\theta'(0)$ ) for different values of  $M$  when  $Pr = 6.2, Bi = 0.2, \lambda = 0.1, \gamma = 0.1, \phi_1 = \phi_2 = 0.02, \sigma = 0.2$  and  $\varepsilon = -1.4$  (shrinking case)

$\gamma$	$f''(0)$	$-\theta'(0)$
-0.1	1.644042983(0.181959638)	0.322093272(0.123449074)
0	1.645073314(0.316328235)	0.181945448(0.118217285)
0.1	1.646137351(0.310556166)	0.181931763(0.11917141)

Note: () Second solution

**Table 6**

Smallest eigenvalues  $\omega_1$  for some values of  $\varepsilon$  when  $\gamma = -0.1, 0, 0.1$

$\gamma$	$\varepsilon$	$\omega_1$	
		First solution	Second solution
-0.1	-1.40	1.138083142	0.547584054
	-1.431	0.888644807	0.8243699211
	-1.4316	0.8463051	0.882158694
0	-1.45	1.295960157	0.577330963
	-1.487	1.10571056	0.805348201
	-1.4953	0.9929989971	0.992103733
0.1	-1.50	1.469789467	0.595870263
	-1.559	1.183102723	0.9511303
	-1.5650	1.07132899	1.07370097

## 5. Conclusion

In this study, an unsteady stagnation point flow involving  $\text{Al}_2\text{O}_3\text{-Cu}/\text{H}_2\text{O}$  hybrid nanofluid was investigated over a convectively heated stretching/shrinking sheet with the effects of suction/injection and MHD. The numerical results were generated using the `bvp4c` routine being operated on MATLAB. The effects of various control parameters such as nanoparticle volume fraction, suction/injection and MHD on the behaviour of the boundary layer flow and heat transfer were examined. We also observed the existence of first and second solutions for certain sets of control parameters in the velocity and temperature profiles, skin friction coefficient and local Nusselt number.

Increment in the copper nanoparticles volume fraction has increased the skin friction coefficient and the local Nusselt number of the said hybrid nanofluid. This showed that when the usual  $\text{Al}_2\text{O}_3/\text{H}_2\text{O}$  nanofluid is converted into  $\text{Al}_2\text{O}_3\text{-Cu}/\text{H}_2\text{O}$  hybrid nanofluid, the heat transfer rate would increase. The addition of suction/injection parameter  $\gamma$  at the boundary condition had stimulated an increase in the velocity profile ( $f'(\eta)$ ) and skin friction coefficient ( $f''(0)$ ). However, there is a considerable rate of heat transfer. The temperature profile increased as the magnitude of suction/injection rises, which can prohibit the exchange of total heat in the hybrid nanofluid. An increase in the magnetohydrodynamic parameter consequently increases the rate of heat transfer since the MHD parameter ( $M$ ) is directly related to the coefficient of the heat transfer rate. A decrease in the thermal boundary layer thickness at the top of the sheet is thus detected. For a certain number of shrinking cases, it is found that dual solutions occur ( $\varepsilon < 0$ ). According to this research, adding a small scale of suction and magnetic field effect to the heat transfer operation in the cooling/heating industries can improve the heat transfer operation.

## Acknowledgements

The author wishes to thank the assistance of the Fundamental Research Grant Scheme (FRGS) under a grant number of FRGS/1/2018/STG06/UNIMAP/02/3 from the Ministry of Education Malaysia.

## Reference

- [1] Mahapatra, T., and A. S. Gupta. "Heat transfer in stagnation-point flow towards a stretching sheet." *Heat and Mass Transfer* 38, no. 6 (2002): 517-521. <https://doi.org/10.1007/s002310100215>
- [2] Fisher, Edwin G. *Extrusion of plastics*. John Wiley & Sons, 1976.
- [3] Miklavčič, M., and C. Wang. "Viscous flow due to a shrinking sheet." *Quarterly of Applied Mathematics* 64, no. 2 (2006): 283-290. <https://doi.org/10.1090/S0033-569X-06-01002-5>
- [4] Wang, C. Y. "Stagnation flow towards a shrinking sheet." *International Journal of Non-Linear Mechanics* 43, no. 5 (2008): 377-382. <https://doi.org/10.1016/j.ijnonlinmec.2007.12.021>
- [5] Roşca, Alin V., and Ioan Pop. "Flow and heat transfer over a vertical permeable stretching/shrinking sheet with a second order slip." *International Journal of Heat and Mass Transfer* 60 (2013): 355-364. <https://doi.org/10.1016/j.ijheatmasstransfer.2012.12.028>
- [6] Ahmed, Waqar, Nor Azwadi Che Sidik, and Yutaka Asako. "Metal Oxide and Ethylene Glycol Based Well Stable Nanofluids for Mass Flow in Closed Conduit." *Journal of Advanced Research in Micro and Nano Engineering* 6, no. 1 (2021): 1-15.
- [7] Sajid, Muhammad Usman, and Hafiz Muhammad Ali. "Thermal conductivity of hybrid nanofluids: a critical review." *International Journal of Heat and Mass Transfer* 126 (2018): 211-234. <https://doi.org/10.1016/j.ijheatmasstransfer.2018.05.021>
- [8] Sarkar, Jahar, Pradyumna Ghosh, and Arjumand Adil. "A review on hybrid nanofluids: recent research, development and applications." *Renewable and Sustainable Energy Reviews* 43 (2015): 164-177. <https://doi.org/10.1016/j.rser.2014.11.023>
- [9] Suresh, S., K. P. Venkitaraj, P. Selvakumar, and M. Chandrasekar. "Synthesis of  $\text{Al}_2\text{O}_3\text{-Cu}/\text{water}$  hybrid nanofluids using two step method and its thermo physical properties." *Colloids and Surfaces A: Physicochemical and Engineering Aspects* 388, no. 1-3 (2011): 41-48. <https://doi.org/10.1016/j.colsurfa.2011.08.005>

- [10] Soltani, Omid, and Mohammad Akbari. "Effects of temperature and particles concentration on the dynamic viscosity of MgO-MWCNT/ethylene glycol hybrid nanofluid: experimental study." *Physica E: Low-dimensional Systems and Nanostructures* 84 (2016): 564-570. <https://doi.org/10.1016/j.physe.2016.06.015>
- [11] Chamkha, Ali J., Sina Sazegar, Esmael Jamesahar, and Mohammad Ghalambaz. "Thermal non-equilibrium heat transfer modeling of hybrid nanofluids in a structure composed of the layers of solid and porous media and free nanofluids." *Energies* 12, no. 3 (2019): 541. <https://doi.org/10.3390/en12030541>
- [12] Mehryan, S. A. M., E. Izadpanahi, M. Ghalambaz, and A. J. Chamkha. "Mixed convection flow caused by an oscillating cylinder in a square cavity filled with Cu-Al<sub>2</sub>O<sub>3</sub>/water hybrid nanofluid." *Journal of Thermal Analysis and Calorimetry* 137, no. 3 (2019): 965-982. <https://doi.org/10.1007/s10973-019-08012-2>
- [13] Sidik, Nor Azwadi Che, Isa Muhammad Adamu, Muhammad Mahmud Jamil, G. H. R. Kefayati, Rizalman Mamat, and G. Najafi. "Recent progress on hybrid nanofluids in heat transfer applications: a comprehensive review." *International Communications in Heat and Mass Transfer* 78 (2016): 68-79. <https://doi.org/10.1016/j.icheatmasstransfer.2016.08.019>
- [14] Akilu, Suleiman, K. V. Sharma, Aklilu Tesfamichael Baheta, and Rizalman Mamat. "A review of thermophysical properties of water based composite nanofluids." *Renewable and Sustainable Energy Reviews* 66 (2016): 654-678. <https://doi.org/10.1016/j.rser.2016.08.036>
- [15] Babu, J. A. Ranga, K. Kiran Kumar, and S. Srinivasa Rao. "State-of-art review on hybrid nanofluids." *Renewable and Sustainable Energy Reviews* 77 (2017): 551-565. <https://doi.org/10.1016/j.rser.2017.04.040>
- [16] Sundar, L. Syam, K. V. Sharma, Manoj K. Singh, and A. C. M. Sousa. "Hybrid nanofluids preparation, thermal properties, heat transfer and friction factor-a review." *Renewable and Sustainable Energy Reviews* 68 (2017): 185-198. <https://doi.org/10.1016/j.rser.2016.09.108>
- [17] Leong, K. Y., KZ Ku Ahmad, Hwai Chyuan Ong, M. J. Ghazali, and Azizah Baharum. "Synthesis and thermal conductivity characteristic of hybrid nanofluids-a review." *Renewable and Sustainable Energy Reviews* 75 (2017): 868-878. <https://doi.org/10.1016/j.rser.2016.11.068>
- [18] Huminic, Gabriela, and Angel Huminic. "Hybrid nanofluids for heat transfer applications-a state-of-the-art review." *International Journal of Heat and Mass Transfer* 125 (2018): 82-103. <https://doi.org/10.1016/j.ijheatmasstransfer.2018.04.059>
- [19] Devi, S. P. Anjali, and S. Suriya Uma Devi. "Numerical investigation of hydromagnetic hybrid Cu-Al<sub>2</sub>O<sub>3</sub>/water nanofluid flow over a permeable stretching sheet with suction." *International Journal of Nonlinear Sciences and Numerical Simulation* 17, no. 5 (2016): 249-257. <https://doi.org/10.1515/ijnsns-2016-0037>
- [20] Devi, S. Suriya Uma, and S. P. Anjali Devi. "Numerical investigation of three-dimensional hybrid Cu-Al<sub>2</sub>O<sub>3</sub>/water nanofluid flow over a stretching sheet with effecting Lorentz force subject to Newtonian heating." *Canadian Journal of Physics* 94, no. 5 (2016): 490-496. <https://doi.org/10.1139/cjp-2015-0799>
- [21] Hayat, Tanzila, and S. Nadeem. "Heat transfer enhancement with Ag-CuO/water hybrid nanofluid." *Results in Physics* 7 (2017): 2317-2324. <https://doi.org/10.1016/j.rinp.2017.06.034>
- [22] Nadeem, S., Nadeem Abbas, and A. U. Khan. "Characteristics of three dimensional stagnation point flow of Hybrid nanofluid past a circular cylinder." *Results in Physics* 8 (2018): 829-835. <https://doi.org/10.1016/j.rinp.2018.01.024>
- [23] Yousefi, Mohammad, Saeed Dinarvand, Mohammad Eftekhari Yazdi, and Ioan Pop. "Stagnation-point flow of an aqueous titania-copper hybrid nanofluid toward a wavy cylinder." *International Journal of Numerical Methods for Heat & Fluid Flow* 28, no. 7 (2018): 1716-1735. <https://doi.org/10.1108/HFF-01-2018-0009>
- [24] Waini, Iskandar, Anuar Ishak, and Ioan Pop. "Unsteady flow and heat transfer past a stretching/shrinking sheet in a hybrid nanofluid." *International Journal of Heat and Mass Transfer* 136 (2019): 288-297. <https://doi.org/10.1016/j.ijheatmasstransfer.2019.02.101>
- [25] Khashi'ie, Najiyah Safwa, Norihan Md Arifin, Roslinda Nazar, Ezad Hafidz Hafidzuddin, Nadiah Wahid, and Ioan Pop. "Magnetohydrodynamics (MHD) axisymmetric flow and heat transfer of a hybrid nanofluid past a radially permeable stretching/shrinking sheet with Joule heating." *Chinese Journal of Physics* 64 (2020): 251-263. <https://doi.org/10.1016/j.cjph.2019.11.008>
- [26] Beavers, Gordon S., and Daniel D. Joseph. "Boundary conditions at a naturally permeable wall." *Journal of Fluid Mechanics* 30, no. 1 (1967): 197-207. <https://doi.org/10.1017/S0022112067001375>
- [27] Andersson, Helge I. "Slip flow past a stretching surface." *Acta Mechanica* 158, no. 1 (2002): 121-125. <https://doi.org/10.1007/BF01463174>
- [28] Wang, C. Y. "Flow due to a stretching boundary with partial slip-an exact solution of the Navier-Stokes equations." *Chemical Engineering Science* 57, no. 17 (2002): 3745-3747. [https://doi.org/10.1016/S0009-2509\(02\)00267-1](https://doi.org/10.1016/S0009-2509(02)00267-1)
- [29] Rusdi, Nadia Diana Mohd, Siti Suzilliana Putri Mohamed Isa, Norihan Md Arifin, and Norfifah Bachok. "Thermal Radiation in Nanofluid Penetrable Flow Bounded with Partial Slip Condition." *CFD Letters* 13, no. 8 (2021): 32-44. <https://doi.org/10.37934/cfdl.13.8.3244>

- [30] Mahabaleshwar, U. S., K. R. Nagaraju, M. A. Sheremet, P. N. Vinay Kumar, and G. Lorenzini. "Effect of mass transfer and MHD induced Navier's slip flow due to a non linear stretching sheet." *Journal of Engineering Thermophysics* 28, no. 4 (2019): 578-590. <https://doi.org/10.1134/S1810232819040131>
- [31] Khan, Ansab Azam, Khairy Zaimi, and Teh Yuan Ying. "Stagnation point flow of Williamson nanofluid towards a permeable stretching/shrinking sheet with a partial slip." *CFD Letters* 12, no. 6 (2020): 39-56. <https://doi.org/10.37934/cfdl.12.6.3956>
- [32] Ebaid, Abdelhalim, Fahd Al Mutairi, and S. M. Khaled. "Effect of velocity slip boundary condition on the flow and heat transfer of Cu-water and TiO<sub>2</sub>-water nanofluids in the presence of a magnetic field." *Advances in Mathematical Physics* 2014 (2014). <https://doi.org/10.1155/2014/538950>
- [33] Bhattacharyya, Krishnendu, Swati Mukhopadhyay, and G. C. Layek. "Slip effects on boundary layer stagnation-point flow and heat transfer towards a shrinking sheet." *International Journal of Heat and Mass Transfer* 54, no. 1-3 (2011): 308-313. <https://doi.org/10.1016/j.ijheatmasstransfer.2010.09.041>
- [34] Aziz, Asim, Yasir Ali, Taha Aziz, and J. I. Siddique. "Heat transfer analysis for stationary boundary layer slip flow of a power-law fluid in a Darcy porous medium with plate suction/injection." *PLoS One* 10, no. 9 (2015): e0138855. <https://doi.org/10.1371/journal.pone.0138855>
- [35] Uwanta, I. J., and M. M. Hamza. "Effect of suction/injection on unsteady hydromagnetic convective flow of reactive viscous fluid between vertical porous plates with thermal diffusion." *International Scholarly Research Notices* 2014 (2014). <https://doi.org/10.1155/2014/980270>
- [36] Bachok, Norfifah, Anuar Ishak, and Ioan Pop. "Boundary layer flow over a moving surface in a nanofluid with suction or injection." *Acta Mechanica Sinica* 28, no. 1 (2012): 34-40. <https://doi.org/10.1007/s10409-012-0014-x>
- [37] Rehman, Sajid, M. Idrees, Rehan Ali Shah, and Zeeshan Khan. "Suction/injection effects on an unsteady MHD Casson thin film flow with slip and uniform thickness over a stretching sheet along variable flow properties." *Boundary Value Problems* 2019, no. 1 (2019): 1-24. <https://doi.org/10.1186/s13661-019-1133-0>
- [38] Li, Botong, Yikai Yang, and Xuehui Chen. "A power-law liquid food flowing through an uneven channel with non-uniform suction/injection." *International Journal of Heat and Mass Transfer* 144 (2019): 118639. <https://doi.org/10.1016/j.ijheatmasstransfer.2019.118639>
- [39] Anuar, Nur Syazana, Norfifah Bachok, Norihan Md Arifin, and Haliza Rosali. "Effect of suction/injection on stagnation point flow of hybrid nanofluid over an exponentially shrinking sheet with stability analysis." *CFD Letters* 11, no. 12 (2019): 21-33. <https://doi.org/10.3390/sym11040522>
- [40] Zainal, Nurul Amira, Roslinda Nazar, Kohilavani Naganthran, and Ioan Pop. "Unsteady MHD stagnation point flow induced by exponentially permeable stretching/shrinking sheet of hybrid nanofluid." *Engineering Science and Technology, an International Journal* 24, no. 5 (2021): 1201-1210. <https://doi.org/10.1016/j.jestch.2021.01.018>
- [41] Daniel, Yahaya Shagaiya, Zainal Abdul Aziz, Zuhaila Ismail, and Faisal Salah. "Thermal radiation on unsteady electrical MHD flow of nanofluid over stretching sheet with chemical reaction." *Journal of King Saud University-Science* 31, no. 4 (2019): 804-812. <https://doi.org/10.1016/j.jksus.2017.10.002>
- [42] Van Gorder, Robert, and K. Vajravelu. "Multiple solutions for hydromagnetic flow of a second grade fluid over a stretching or shrinking sheet." *Quarterly of Applied Mathematics* 69, no. 3 (2011): 405-424. <https://doi.org/10.1090/S0033-569X-2011-01211-1>
- [43] Tian, Xi-Yan, Ben-Wen Li, and Zhang-Mao Hu. "Convective stagnation point flow of a MHD non-Newtonian nanofluid towards a stretching plate." *International Journal of Heat and Mass Transfer* 127 (2018): 768-780. <https://doi.org/10.1016/j.ijheatmasstransfer.2018.07.033>
- [44] Dhanai, Ruchika, Puneet Rana, and Lokendra Kumar. "Multiple solutions of MHD boundary layer flow and heat transfer behavior of nanofluids induced by a power-law stretching/shrinking permeable sheet with viscous dissipation." *Powder Technology* 273 (2015): 62-70. <https://doi.org/10.1016/j.powtec.2014.12.035>
- [45] Khan, Ansab Azam, Khairy Zaimi, Suliadi Firdaus Sufahani, and Mohammad Ferdows. "MHD flow and heat transfer of double stratified micropolar fluid over a vertical permeable shrinking/stretching sheet with chemical reaction and heat source." *Journal of Advanced Research in Applied Sciences and Engineering Technology* 21, no. 1 (2020): 1-14. <https://doi.org/10.37934/araset.21.1.114>
- [46] Khan, Ansab Azam, Khairy Zaimi, Suliadi Firdaus Sufahani, and Mohammad Ferdows. "MHD Mixed Convection Flow and Heat Transfer of a Dual Stratified Micropolar Fluid Over a Vertical Stretching/Shrinking Sheet With Suction, Chemical Reaction and Heat Source." *CFD Letters* 12, no. 11 (2020): 106-120. <https://doi.org/10.37934/cfdl.12.11.106120>
- [47] Ashgar, Adnan, and Teh Yuan Ying. "Three dimensional MHD hybrid nanofluid Flow with rotating stretching/shrinking sheet and Joule heating." *CFD Letters* 13, no. 8 (2021): 1-19. <https://doi.org/10.37934/cfdl.13.8.119>

- [48] Akaje, T. W., and B. I. Olajuwon. "Impacts of Nonlinear thermal radiation on a stagnation point of an aligned MHD Casson nanofluid flow with Thompson and Troian slip boundary condition." *Journal of Advanced Research in Experimental Fluid Mechanics and Heat Transfer* 6, no. 1 (2021): 1-15.
- [49] Katagiri, Masakazu. "Unsteady magnetohydrodynamic flow at the forward stagnation point." *Journal of the Physical Society of Japan* 27, no. 6 (1969): 1662-1668. <https://doi.org/10.1143/JPSJ.27.1662>
- [50] Pavlov, K. B. "Magnetohydrodynamic flow of an incompressible viscous fluid caused by deformation of a plane surface." *Magnitnaya Gidrodinamika* 4, no. 1 (1974): 146-147.
- [51] Takhar, Harmindar S., Ashok K. Singh, and Girishwar Nath. "Unsteady MHD flow and heat transfer on a rotating disk in an ambient fluid." *International Journal of Thermal Sciences* 41, no. 2 (2002): 147-155. [https://doi.org/10.1016/S1290-0729\(01\)01292-3](https://doi.org/10.1016/S1290-0729(01)01292-3)
- [52] Zainal, Nurul Amira, Roslinda Nazar, Kohilavani Naganthran, and Ioan Pop. "MHD flow and heat transfer of hybrid nanofluid over a permeable moving surface in the presence of thermal radiation." *International Journal of Numerical Methods for Heat & Fluid Flow* 31, no. 3 (2020): 858-879. <https://doi.org/10.1108/HFF-03-2020-0126>
- [53] Jamaludin, Anuar, Kohilavani Naganthran, Roslinda Nazar, and Ioan Pop. "MHD mixed convection stagnation-point flow of Cu-Al<sub>2</sub>O<sub>3</sub>/water hybrid nanofluid over a permeable stretching/shrinking surface with heat source/sink." *European Journal of Mechanics-B/Fluids* 84 (2020): 71-80. <https://doi.org/10.1016/j.euromechflu.2020.05.017>
- [54] Mallick, B., and J. C. Misra. "Peristaltic flow of Eyring-Powell nanofluid under the action of an electromagnetic field." *Engineering Science and Technology, an International Journal* 22, no. 1 (2019): 266-281. <https://doi.org/10.1016/j.jestch.2018.12.001>
- [55] Smith, F. T. "Steady and unsteady boundary-layer separation." *Annual Review of Fluid Mechanics* 18, no. 1 (1986): 197-220. <https://doi.org/10.1146/annurev.fl.18.010186.001213>
- [56] Takabi, Behrouz, and Saeed Salehi. "Augmentation of the heat transfer performance of a sinusoidal corrugated enclosure by employing hybrid nanofluid." *Advances in Mechanical Engineering* 6 (2014): 147059. <https://doi.org/10.1155/2014/147059>
- [57] Ghalambaz, Mohammad, Natalia C. Roşca, Alin V. Roşca, and Ioan Pop. "Mixed convection and stability analysis of stagnation-point boundary layer flow and heat transfer of hybrid nanofluids over a vertical plate." *International Journal of Numerical Methods for Heat & Fluid Flow* 30, no. 7 (2019): 3737-3754. <https://doi.org/10.1108/HFF-08-2019-0661>
- [58] Zainal, Nurul Amira, Roslinda Nazar, Kohilavani Naganthran, and Ioan Pop. "Unsteady stagnation point flow of hybrid nanofluid past a convectively heated stretching/shrinking sheet with velocity slip." *Mathematics* 8, no. 10 (2020): 1649. <https://doi.org/10.3390/math8101649>
- [59] Dzulkipli, Nor Fadhilah, Norfifah Bachok, Nor Azizah Yacob, Norihan Md Arifin, and Haliza Rosali. "Unsteady stagnation-point flow and heat transfer over a permeable exponential stretching/shrinking sheet in nanofluid with slip velocity effect: A stability analysis." *Applied Sciences* 8, no. 11 (2018): 2172. <https://doi.org/10.3390/app8112172>
- [60] Mahapatra, Tapas Ray, and Samir Kumar Nandy. "Slip effects on unsteady stagnation-point flow and heat transfer over a shrinking sheet." *Meccanica* 48, no. 7 (2013): 1599-1606. <https://doi.org/10.1007/s11012-012-9688-1>
- [61] Shampine, Lawrence F., Ian Gladwell, and S. Thompson. *Solving ODEs with MATLAB*. Cambridge University Press, 2003. <https://doi.org/10.1017/CBO9780511615542>
- [62] Ishak, Anuar. "MHD boundary layer flow due to an exponentially stretching sheet with radiation effect." *Sains Malaysiana* 40, no. 4 (2011): 391-395.
- [63] Sarkar, Jahar, Pradyumna Ghosh, and Arjumand Adil. "A review on hybrid nanofluids: recent research, development and applications." *Renewable and Sustainable Energy Reviews* 43 (2015): 164-177. <https://doi.org/10.1016/j.rser.2014.11.023>
- [64] Oztop, Hakan F., and Eiyad Abu-Nada. "Numerical study of natural convection in partially heated rectangular enclosures filled with nanofluids." *International Journal of Heat and Fluid Flow* 29, no. 5 (2008): 1326-1336. <https://doi.org/10.1016/j.ijheatfluidflow.2008.04.009>